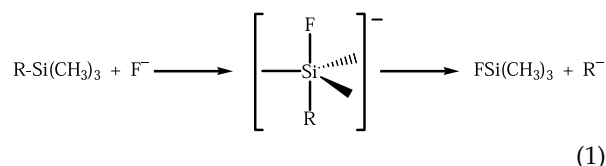# Fluorotrimethylsilane Affinities of Anionic Nucleophiles: A Study of Fluoride-Induced Desilylation

Ian H. Krouse and Paul G. Wenthold

Department of Chemistry, Purdue University, West Lafayette, Indiana, USA

In this study, preparation and decomposition of five novel pentavalent fluorosiliconates, $RSi(CH_3)_3F^-$ (R = CH_3CH_2O, CF_3CH_2O, $(CH_3)_2CHO$, $(CH_3)_3SiO$, and $(CH_3)_3SiNH$) is used to investigate the process of fluoride-induced desilylation. The siliconates were characterized by collision-induced dissociation and energy-resolved mass spectrometry. Decomposition of $RSi(CH_3)_3F^-$ leads to loss of the nucleophile R^- and $FSi(CH_3)_3$, except in the case of $(CH_3)_3SiNHSi(CH_3)_3F^-$, where HF loss is also observed. Ion affinities for $FSi(CH_3)_3$ have been measured for all five nucleophiles, and compare well with computational predictions. The observed trend of the bond dissociation energies resembles the trend of ΔH_{acid} values for the corresponding conjugate acids, RH. Additionally, this data has been incorporated with existing thermochemistry to derive fluoride affinities for four of the silanes (R = CH_3CH_2O, $(CH_3)_2CHO$, $(CH_3)_3SiO$, and $(CH_3)_3SiNH$). We use the fluoride affinity of the silanes and the $FSi(CH_3)_3$ affinity of the departing nucleophilic anion to assess the feasibility of fluoride-induced desilylation of the silanes examined in this work.   (J Am Soc Mass Spectrom 2005, 16, 697–707) © 2005 American Society for Mass Spectrometry

Desilylation via halogen addition is a common synthetic approach [1]. Indeed, silyl moieties are often used as protecting groups because of the ease of their removal with fluoride and chloride [2, 3]. Extension of this Group 14 chemistry has led to the process of fluoride-induced destannylation, also well-known within the literature [4, 5]. Fluoride-induced desilylation is particularly useful because the formation of the strong Si—F bond is a highly selective procedure [1]. In the gas phase, fluoride-induced desilylation, pioneered by DePuy et al. [6, 7], is also very functional and has been used extensively to generate carbanions regioselectively via the general reaction shown in eq 1.

$$R\text{-}Si(CH_3)_3 + F^- \longrightarrow \left[\begin{array}{c} F \\ | \\ \text{---} Si \cdots \text{''} \\ | \\ R \end{array} \right]^- \longrightarrow FSi(CH_3)_3 + R^-$$

(1)

In particular, fluoride-induced desilylation has been used to generate various cyclic [8, 9] and alkenyl ions [10] in the gas phase, and overviews of the reactivity are available [7, 11]. By using the reaction of fluoride with silanes, Kass and coworkers have prepared several anions for characterization, including acetamide enolate [12], cyclopropenyl derivatives [8, 13], and cubyl anion

[14]. In addition, reaction of fluoride with disilanes causes cleavage of Si—Si bonds to produce silyl anions [15, 16]. Lastly, a variation of fluoride-induced desilylation involving the reaction of trimethylsilyl substituted anions has also been used to prepare open-shell anions of biradicals, triradicals, and beyond [9, 17–22].

In general, fluoride-induced desilylation is believed to occur through a fluorinated pentavalent siliconate intermediate, followed by elimination of the neutral silane (eq 1), analogous to an S_N2 reaction in carbon systems [23]. However, because third row and lower main-group elements (e.g., P, S, Cl) readily undergo hypervalent bonding [24], the pentavalent siliconate is a stable intermediate in the reaction and can, in many cases, be observed [25–28]. Because of their stability, siliconates are often used in fundamental studies of hypervalency [26, 29–32], as well as in numerous theoretical [33, 34] and experimental [7, 29, 35–40] studies.

In continuation of our interest in inorganic main group gas-phase chemistry [27, 28], we have studied the formation and decomposition of a series of pentavalent fluorosiliconates, $RSi(CH_3)_3F^-$. Although there has been some thermochemical characterization of pentavalent siliconates, the effects of substitution are not well known [41]. Chloride and fluoride affinities have been reported for some silanes [42–44], but there are few other experimental nucleophilic affinities. Most negative ion studies of silanes have focused upon reactivity [45–49] with few studies looking specifically at silicon-related ion thermochemistry [27, 28, 43, 50].

In this work, pentavalent siliconates are prepared by

the termolecular addition of fluoride to the silane, giving an adduct $RSi(CH_3)_3F^-$. Upon collisional activation, the siliconate decomposes by loss of nucleophile R^-, leaving fluorotrimethylsilane. We use energy-resolved collision-induced dissociation (CID) of the pentavalent siliconates to determine enthalpies for binding of $FSi(CH_3)_3$ to the anions. The binding energy of the silane to nucleophiles is important to know because it is the energy that must be overcome to form ions through fluoride-induced desilylation of trimethylsilyl substituted silanes.

The silanes examined in this study include those with alkoxy ($R = CH_3O$, $(CH_3)_2CHO$, CH_3CH_2O, and CF_3CH_2O), siloxy [$(CH_3)_3SiO$] and amino [$(CH_3)_3SiNH$] substituents. Whereas it is expected that the alkoxy moieties will have roughly the same affinity for $FSi(CH_3)_3$, the 2,2,2-trifluoroethoxy substituent is expected to have a smaller binding affinity because of the electron-withdrawing effect of the trifluoromethyl group. Although isopropoxy- and 2,2,2-trifluoroethoxytrimethylsilane have limited synthetic use, ethoxytrimethylsilane is an important polysiloxane precursor and is used to prepare esters, ethers and glycols [51, 52]. Hexamethyldisiloxane and 1,1,1,3,3,3-hexamethyldisilazane (HMDS) are isoelectronic, so it is of interest to determine the differences in reactivity and thermochemistry between the oxygen and the nitrogen systems. Hexamethyldisiloxane is used extensively in synthesis [53, 54] and polymerizations, whereas $(CH_3)_3SiNHSi(CH_3)_3$ (and its derivatives) are the primary species used as bulky amido ligands. HMDS has also been used to silylate glass capillary columns for chromatography [55]. In general, the synthetic utility of both $(CH_3)_3SiOSi(CH_3)_3$ and $(CH_3)_3SiNHSi(CH_3)_3$ is widespread [52].

Experimental

Instrumental Description and Data Analysis

All gas-phase ion/molecule reactions were carried out using a flowing afterglow-triple quadrupole mass spectrometer that has been described previously [56, 57]. Fluoride was prepared by 70 eV electron ionization of neutral fluorine gas (5% in He, Spectra Gases Inc., Branchburg, NJ) and carried by helium buffer gas (0.400 Torr, flow(He) = 190 STP cm^3/s) through the flow tube, where it was allowed to react with vapors from silanes added through micrometering valves. In order to increase yield of ions, the reactions were carried out in the presence of wet THF [58].

Ions generated in the flow tube were sampled through a 1 mm nose cone orifice into a differentially pumped region, where they were analyzed using a triple quadrupole mass filter (EXTREL, Inc. Pittsburgh, PA). Collision-induced dissociation was carried out by mass selecting the reactant ion of interest with the first quadrupole and injecting the ion into the second quadrupole, which serves as a collision cell containing argon as the target gas. The CID collision energy was controlled by the pole offset voltage, and the absolute energy origin was established by using retarding potential analysis. The uncertainty in the absolute energy scale is estimated to be ± 0.15 eV in the laboratory frame.

Product ions were mass analyzed with the third quadrupole and detected with a channeltron particle detector operated in pulsed-counting mode. Cross sections for CID, σ, are calculated using $I/I_0 = \sigma Nl$, where I and I_0 are the intensities of the product and reactant ions, respectively, N is the number density of the target, and l is the effective collision path length, calibrated to be 24 ± 4 cm [57] by using the reaction of $Ar^+ + D_2$, which has a well-established cross section [59]. Cross sections were measured as a function of target pressure and extrapolated to zero pressure, single collision conditions. Cross sections were modeled with the exponential expression shown in eq 2 [60–63], where E is the center-of-mass collision energy of the reactant ion, g_i is the fraction of the ions with internal energy E_i, E_0 is the threshold energy for dissociation, n is a parameter that reflects the energy deposition in the collision [64], and σ_0 is a scaling factor. The data are modeled by adjusting the parameters to fit the steeply rising portion of the appearance curve(s) directly past the threshold. Convoluted in the fit are the ion kinetic energy distributions, approximated as a Gaussian with a 1.5 eV (laboratory frame) full-width at half-maximum, and a Doppler broadening function to account for motion of the target. The factor P_i is the probability for ion dissociation with the given internal energy, calculated from RRKM theory.

$$\sigma(E) = \frac{\sigma_0 \sum_i P_i g_i (E + E_i - E_0)^n}{E} \qquad (2)$$

For direct dissociation reactions, product-like transition states were assumed, corresponding to the phase-space limit [65]. Activation entropies for direct dissociation reactions are generally +10–20 cal/mol · K, indicating loose transition states. Data analysis and modeling were carried out using the CRUNCH 4D program developed by Armentrout and coworkers [59, 60, 65–67]. In the absence of reverse activation barriers, threshold energies can be equated with 0 K ΔE values and converted to 298 K bond dissociation enthalpies by using the integrated heat capacities of reactants and products. Uncertainties in enthalpy values were calculated by statistical combination of the uncertainty in the absolute energy scale for the experiment, the standard deviation of values obtained from replicate experimental trials, and uncertainty from error in the transition state. Error in the transition state was estimated as the change in the dissociation energy that results when the frequencies of the transition state are scaled to change the activation entropy by ±2 cal/mol · K. In the case of multiple product channels, the transition state error was determined separately for each channel, and then
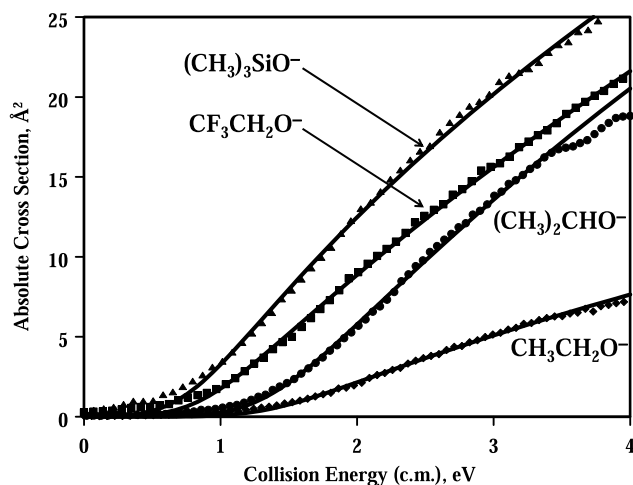
Figure 1. Energy resolved absolute cross sections for the decomposition of (CH$_3$)$_3$SiOSi(CH$_3$)$_3$F$^-$, CF$_3$CH$_2$OSi(CH$_3$)$_3$F$^-$, (CH$_3$)$_2$CHOSi(CH$_3$)$_3$F$^-$, and CH$_3$CH$_2$OSi(CH$_3$)$_3$F$^-$. The triangles are cross sections for formation of (CH$_3$)$_3$SiO$^-$. The squares are cross sections for formation of CF$_3$CH$_2$O$^-$. The circles are cross sections for formation of (CH$_3$)$_2$CHO$^-$, and the diamonds are cross sections for formation of (CH$_3$)$_3$SiO$^-$. The solid lines are the fully convoluted fits for the reaction channels, obtained with the modeling parameters given in Table 1.

combined into an overall transition state error for all pathways. Uncertainty for the parameter n was determined in an analogous fashion.

Materials

Unless otherwise indicated, reagents were used as received without further purification. Helium gas was purified via a liquid nitrogen trap containing molecular sieves. All silanes were distilled, dried over molecular sieves, stored at −10 °C and freeze-pump-thawed prior to use. Wet THF was prepared by adding approximately 2% H$_2$O to THF (Mallinckrodt, Phillipsburg, NJ), and freeze-pump-thawed prior to use. All silanes except 2,2,2-trifluoroethoxytrimethylsilane were commercially obtained (Aldrich, Milwaukee, WI). A lab sample of 2,2,2-trifluoroethoxytrimethylsilane was prepared as described by Kirchmeier and co-workers [68].

Computational Methods

Rotational constants and frequencies of reactants, transition states, and products, required to calculate the internal energies of the ion and the RRKM dissociation rates, were calculated at the B3LYP/6-31 + G* level of theory using Gaussian 03 [69]. Additionally, geometries, energies, and frequencies for reactants and products related to the fluoride adduct of HMDS were calculated at the MP2/6-31 + G* level of theory. Absolute energies, geometries and frequencies are available upon request. Bond dissociation energies are not corrected for basis set superposition error.

Results

The following section describes the results of the studies of the collision-induced decomposition of the fluoride adducts of the five silanes. General reactivity for the process R$_3$SiA + Nu$^-$ has been described in detail in the review by Damrauer and Hankin [70], so we have focused this work on the formation of fluoride adducts and their properties. All reactions were carried out by the termolecular addition of fluoride ion to the silanes in the presence of wet THF. Although the wet THF is not required, it promoted larger yields of ionic products for all of the silane reactions, presumably by solvating the fluoride. None of the fluorosiliconates prepared from this study have been reported previously. For most of the oxygenated siliconates, RSi(CH$_3$)$_3$F$^-$ (R = CH$_3$CH$_2$O, CF$_3$CH$_2$O, (CH$_3$)$_2$CHO and (CH$_3$)$_3$SiO), dissociation is dominated by the loss of R$^-$. Minor channels were observed in these dissociations, but they are less than 2% of the total product and therefore should not significantly affect the formation of the major product. These minor channels were ignored in the analyses. The fits of the energy-resolved cross sections for dissociation of the alkoxy siliconates are shown as solid lines in Figure 1. Modeling parameters for each of the single pathway reactions are given in Table 1. For these reactions, the cross section data were modeled by assuming loose, dissociative variational transition states, typical for direct cleavage processes [65]. Overall uncertainties were determined as described in the Experimental section. The following sections describe the specific results for each siliconate ion.

Reaction of F$^-$ and Ethoxytrimethylsilane, CH$_3$CH$_2$OSi(CH$_3$)$_3$

The ethoxyfluorotrimethylsiliconate anion, CH$_3$CH$_2$O Si(CH$_3$)$_3$F$^-$ (m/z 137) is formed by addition of fluoride to CH$_3$CH$_2$OSi(CH$_3$)$_3$ (eq 3a). Upon CID, the ion loses FSi(CH$_3$)$_3$ to give CH$_3$CH$_2$O$^-$ (m/z 45) as the major ionic product (eq 3b). Deprotonated fluorotrimethylsilane (FSi(CH$_3$)$_2$CH$_2$$^-$, m/z 91) was also observed upon CID, but accounted for less than 2% of the ionic products over the entire energy range and was ignored. The

Table 1. Modeling parameters[a] and calculated values for dissociation of siliconate species, RSi(CH$_3$)$_3$F$^-$

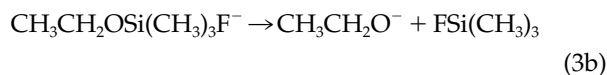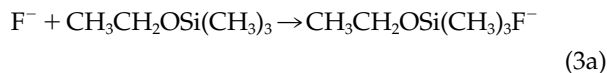| R	ΔH$_{298}$[b]	n[bc]	Calculated value DH$_{298}$(R$^-$ − FSi(CH$_3$)$_3$)[d]
CH$_3$CH$_2$O	31.4 ± 1.2	1.7 ± 0.1	29.6 (39.4)
CF$_3$CH$_2$O	23.8 ± 1.2	1.7 ± 0.2	21.6 (30.7)
(CH$_3$)$_2$CHO	32.1 ± 1.8	1.5 ± 0.1	26.4 (37.1)
(CH$_3$)$_3$SiO	21.4 ± 2.1	1.6 ± 0.1	20.0 (27.7)

[a]Fitting parameters from eq 2, as described in the text. Energy values in kcal/mol.
[b]Uncertainty as described in experimental section.
[c]Exponent in eq 2.
[d]Calculated enthalpies for the reaction computed at the B3LYP/6-31 + G* and (MP2/6-31 + G*) levels of theory.

energy-resolved cross sections for formation of ethoxide are shown in Figure 1. The bond dissociation enthalpy of ethoxide to fluorotrimethylsilane was determined by the modeling the cross section to be 1.36 ± 0.05 eV (31.4 ± 1.2 kcal/mol).

$$F^- + CH_3CH_2OSi(CH_3)_3 \rightarrow CH_3CH_2OSi(CH_3)_3F^-$$

(3a)

$$CH_3CH_2OSi(CH_3)_3F^- \rightarrow CH_3CH_2O^- + FSi(CH_3)_3$$

(3b)

Reaction of F^- and 2,2,2-Trifluoroethoxytrimethylsilane, $CF_3CH_2OSi(CH_3)_3$

The 2,2,2-trifluoroethoxyfluorotrimethylsiliconate anion, $CF_3CH_2OSi(CH_3)_3F^-$ (m/z 191), is formed by direct addition of fluoride to the corresponding silane. CID of the adduct gave fluorotrimethylsilane and the 2,2,2-trifluoroethoxy anion, $CF_3CH_2O^-$ (m/z 99). There was also some CF_3^- ($<2\%$) observed at higher energies, presumably by sequential loss from $CF_3CH_2O^-$, but it was not included in the analysis. The energy-resolved cross sections for this process are given in Figure 1. Modeling the cross sections gave a bond dissociation energy of 1.03 ± 0.05 eV (23.8 ± 1.2 kcal/mol, Table 1).

Reaction of F^- with Isopropoxytrimethylsilane, $(CH_3)_2CHOSi(CH_3)_3$

The fluoride adduct of isopropoxytrimethylsilane, $(CH_3)_2CHOSi(CH_3)_3F^-$ (m/z 151), was prepared by the reaction of fluoride and the silane. Dissociation gave $(CH_3)_2CHO^-$ (m/z 59) as the major ionic product, with a small amount of ethoxy anion (m/z 45) from sequential dissociation of the isopropoxide, accounting for $<2\%$ of the total of ionic products. The energy-resolved cross sections for the formation of $(CH_3)_2CHO^-$ ion are shown in Figure 1. Modeling the cross sections gives a bond dissociation energy of isopropoxide to fluorotrimethylsilane of 1.39 ± 0.08 eV (32.1 ± 1.8 kcal/mol, Table 1).

Reaction of F^- with Hexamethyldisiloxane, $(CH_3)_3SiOSi(CH_3)_3$

Brauman and co-workers [71] have previously shown that reaction of hexamethyldisiloxane with fluoride in an ICR can be used to generate trimethylsiloxide. In the higher-pressure conditions of the flowing afterglow, the adduct $(CH_3)_3SiOSi(CH_3)_3F^-$ (m/z 181) is also formed. Upon CID, the adduct loses fluorotrimethylsilane leaving trimethylsiloxide, $(CH_3)_3SiO^-$ (m/z 89) as the major product. A very small amount of HF loss is also observed, giving $(CH_3)_3SiOSi(CH_3)_2CH_2^-$ (m/z 161). Cross sections for formation of $(CH_3)_3SiO^-$ are shown in Figure 1. The bond dissociation energy of trimethylsiloxide to fluorotrimethylsilane was found to be 0.93 ± 0.09 eV (21.4 ± 2.1 kcal/mol, Figure 1, Table 1).

Reaction of F^- with Methoxytrimethylsilane, $CH_3OSi(CH_3)_3$

Decomposition of fluorotrimethylmethoxysiliconate, $CH_3OSi(CH_3)_3F^-$ was also investigated. The ion was prepared using two separate approaches, either by addition of methoxide to fluorotrimethylsilane or by addition of fluoride to methoxytrimethylsilane. Similar results were obtained for the two generation methods. The adduct undergoes CID at 25 eV (lab) by loss of fluorotrimethylsilane ($\sim20\%$), loss of methanol ($\sim70\%$) and loss of methane ($\sim10\%$). Surprisingly, loss of methanol was the major pathway, unlike all of the other $RSi(CH_3)_3F^-$ systems that gave predominantly loss of $FSi(CH_3)_3$. Although it is in principle possible to model a system with three channels, because of the dissimilarity between the dissociation of this ion and the other alkoxysiliconates, it was not examined further.

Reaction of F^- with 1,1,1,3,3,3-Hexamethyldisilazane, $(CH_3)_3SiNHSi(CH_3)_3$

The fluoride adduct of HMDS, $(CH_3)_3SiNHSi(CH_3)_3F^-$ (m/z 180), was formed by direct addition of fluoride to the disilazane. Upon collisional activation, the adduct dissociated through two major pathways and one minor channel. The two major pathways were loss of $FSi(CH_3)_3$ to form $(CH_3)_3SiNH^-$ (m/z 88) and loss of HF to give hexamethyldisilazide, $(CH_3)_3SiNSi(CH_3)_3^-$ (m/z 160). Formation of hexamethyldisilazide by deprotonation with fluoride in an ICR spectrometer has been reported previously [49, 72]. A very small amount of methane loss was also observed, but this pathway accounted for less than 1% of the total reaction and was not considered further. Energy-resolved cross sections for two major dissociation channels are shown in Figure 2. At high energies (>1 eV), loss of $FSi(CH_3)_3$ is the dominant pathway.

The competitive dissociation was modeled by assuming that both processes proceed by direct dissociation with product-like, variational transition states in the phase space limit (Figure 2). Attempts to model the data by using a tight transition state for one of the channels gave significantly poorer fits to the data. Therefore, if it assumed that at least one of the pathways proceeds by direct dissociation, then the best results are obtained by treating both pathways in this fashion. Modeling of the two pathways gave similar dissociation barriers. The affinity of $FSi(CH_3)_3$ to $(CH_3)_3SiNH^-$ was found to be 1.36 ± 0.10 eV (31.4 ± 2.3 kcal/mol) and the barrier for loss of HF was 1.41 ± 0.13 eV (32.5 ± 2.9 kcal/mol, Table 2).

The fact that both channels proceed by loose, product-like transition states requires that there is a mixture of ions, or that there is a double-well potential surface for the dissociation with a low energy barrier separating the two minima. Changing the source conditions does not affect the branching ratios for the dissociation, suggesting (al-
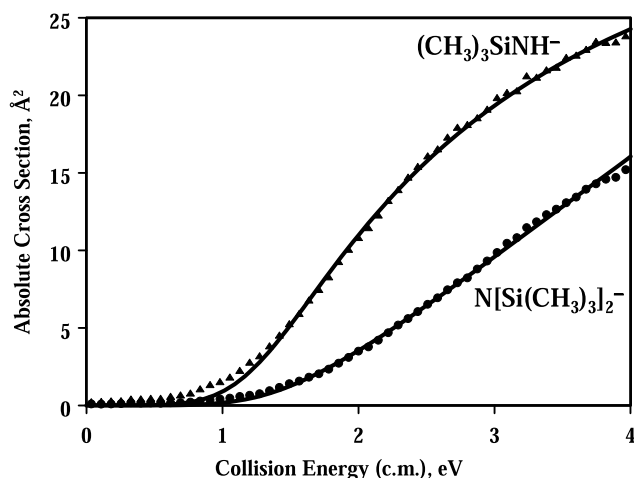
Figure 2. Energy resolved cross sections for the decomposition of $(CH_3)_3SiNHSi(CH_3)_3F^-$. The triangles are cross sections for formation of $(CH_3)_3SiNH^-$ (and loss of $FSi(CH_3)_3$). The circles are cross sections for formation of $(CH_3)_3SiNSi(CH_3)_3^-$ and loss of HF. The solid lines are the fully convoluted fits for the two reaction pathways. Modeling parameters are given in Table 2. The data were fit over the range of 1.4–4.0 eV.

though not requiring) that they do not originate from a discrete ion mixture. However, we have recently shown [28] that the transition states for channels originating from double-well potentials reflect the exit channel properties when the barrier that separates the minima is much lower than the dissociation energy [73, 74], such that the dissociation appears to be arising from distinct reactants. Computational evidence supporting the double-well potential picture is presented in the next section.

Computational Results

Structures and frequencies for the pentavalent siliconates and CID products were computed at the B3LYP/6-31 + G* level of theory. Valence-Shell Elec-

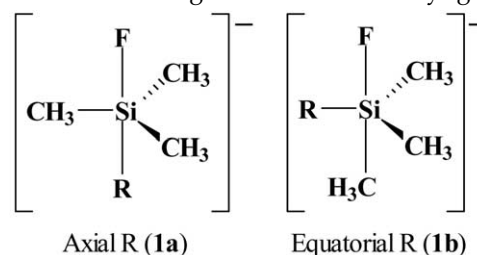**Table 2.** Thermochemical parameters[a] for the CID of $(CH_3)_3SiNHSi(CH_3)_3F^-$

Reactant ion[b] $(CH_3)_3SiNHSi(CH_3)_3F^-$ (2b)	
$DH_{298}((CH_3)_3SiNH^- — Si(CH_3)_3F)$	31.4 ± 2.3 kcal/mol
Barrier for HF loss	32.5 ± 2.9 kcal/mol
n[c]	1.4 ± 0.1
$\Delta S^{\ddagger}(FSi(CH_3)_3$ loss$)$	22.6 cal/mol · K
$\Delta S^{\ddagger}$ (HF loss)	22.4 cal/mol · K
Reactant ion[b] $(CH_3)_3SiNSi(CH_3)_3$—HF (2d)	
$DH_{298}((CH_3)_3SiNH^- — Si(CH_3)_3F)$	27.9 ± 2.5 kcal/mol
Barrier for HF loss	29.3 ± 1.8 kcal/mol
n[c]	1.4 ± 0.1
$\Delta S^{\ddagger}$ ($FSi(CH_3)_3$ loss)	10.7 cal/mol · K
$\Delta S^{\ddagger}$ (HF loss)	10.5 cal/mol · K

[a]Activation barriers correspond to ΔH_{298}.
[b]Data obtained by modeling cross sections for CID of fluoride adduct of $(CH_3)_3SiNHSi(CH_3)$. Modeling assumes that losses of $FSi(CH_3)_3$ and HF both occur via loose (variational) transition states. Structure of adduct is unknown, so fitting parameters for both reactant ions are reported as described in the text.
[c]Exponent in eq 2.

tron-Pair Repulsion (VSEPR) rules predict that pentacoordinate systems should have the smallest substituents in the axial position, and larger substituents in the equatorial positions. Thus, the fluorine substituents prefer the axial position in the lowest energy geometries. However, in the cases of the oxysubstituted siliconates $(CH_3CH_2OSi(CH_3)_3F^-$, $CF_3CH_2OSi(CH_3)_3F^-$, $(CH_3)_2CHOSi(CH_3)_3F^-$, and $(CH_3)_3SiOSi(CH_3)_3F^-)$, the lowest energy structures also have the alkoxy substituents in the axial positions (Table 3). Calculated energy differences between the axial (**1a**) and equatorial (**1b**) geometries are typically 3–4 kcal/mol. Kass and coworkers have previously shown that bulky substituents tend to occupy the axial position in pentavalent siliconates [75], and it has also been suggested that the substituents may prefer the axial position because they are more electronegative than the methyl groups [76].

Axial R (**1a**)　　　Equatorial R (**1b**)

Alternatively, for the fluoride adduct of HMDS the lowest energy structure has the $(CH_3)_3SiNH$ substituent occupying an equatorial position (**2b**), as opposed to the axial (**2a**). The species $(CH_3)_3SiNHSi(CH_3)_3F^-$ adopts a structure in which the amino hydrogen and the fluoride are *anti* to one another. The structure where the amino H and F are *syn* to one another is calculated to be 4.1 kcal/mol higher in energy (**2c**). The fitting parameters shown in the top half of Table 2 were obtained using the frequencies for ion (**2b**). The proton-bound HF cluster of the anion $(CH_3)_3SiNSi(CH_3)_3^-$ (**2d**) was also considered as a possible reactant. This structure was found to be 3.8 kcal/mol higher in energy at the B3LYP/6-31 + G* level of theory, and 6.3 kcal/mol higher in energy at the MP2/6-31 + G* level of theory. Attempts to calculate the alternate hydrogen-bonded structure consisting of fluoride bound to HMDS were unsuccessful, and always led to structure (**2d**). This is not surprising because HMDS is ca. 15 kcal/mol more acidic than HF [49].

Overall, the calculations predict (**2b**) to be the lowest energy structure. However, given the calculated enthalpy differences between (**2b**) and (**2d**), the population of (**2d**) at equilibrium could be anywhere from significant to negligible. B3LYP/6-31 + G* free energies (298 K) for (**2b**) and (**2d**) suggest that there is an almost equal amount of (**2b**) and (**2d**) (free energies of (**2b**) to (**2d**) are within 0.02 kcal/mol), whereas MP2/6-31 + G* free energies indicate a much smaller equilibrium constant (K ∼ 0.01) favoring (**2b**). Thus, calculations suggest that there may be a significant amount of each species present as a mixture. Because the energies of (**2b**) and (**2d**) are sufficiently close

Table 3. Computed absolute and relative enthalpies for isomers of RSi(CH₃)₃F⁻

R	Isomer[a]	Absolute enthalpy[b]	Relative enthalpy[c]
CH₃CH₂O	Axial	−663.483151	0.0
	Equatorial	−663.477675	3.4
CF₃CH₂O	Axial	−961.264965	0.0
	Equatorial	−961.258255	4.2
(CH₃)₂CHO	Axial	−702.772153	0.0
	Equatorial	−702.768000	2.6
(CH₃)₃SiO	Axial	−993.542478	0.0
	Equatorial	−993.537280	3.3
(CH₃)₃SiNH[d]	B3LYP/6–31+G* Enthalpies		
	Axial (**2a**)	−973.608980	5.8
	Equatorial (*trans*) (**2b**)	−973.618284	0.0
	Equatorial (*cis*) (**2c**)	−973.611768	4.1
	HF cluster (**2d**)	−973.612276	3.8
	MP2/6-31+G* Enthalpies[e]		
	Equatorial (*trans*) (**2b**)	−971.238724	0.0
	HF cluster (**2d**)	−971.228682	6.3

[a]Axial/equatorial isomers of RSi(CH₃)₃F⁻ as discussed in the text.
[b]Values in hartrees.
[c]Values in kcal/mol.
[d]Isomers of (CH₃)₃SiNHSi(CH₃)₃F⁻ as discussed in the text and Figure 3.
[e]Computationally expensive MP2/6-31 + G* calculations were only done on selected species.

given the accuracy of the calculation, we have also modeled the data assuming structure (**2d**) as the reactant (bottom half of Table 2). With this reactant, slightly lower dissociation energies are obtained. It is possible that the actual ion population is a mixture of the two structures. In that case, contributions due to dissociation of the higher energy isomer may lead to a slightly lower energy threshold, and therefore lead to an apparent dissociation energy that is lower than that required for the lowest energy reactant. However, because the cross sections near threshold are not included in the fit, the effect of the high energy isomers will be minimal.

Axial (**2a**)   Equatorial (H,F *anti*) (**2b**)

Equatorial (H,F *syn*) (**2c**)   HF Cluster (**2d**)

We have also calculated the structure of the hexamethyldisilazide anion, (CH₃)₃SiNSi(CH₃)₃⁻. At the B3LYP/6-31 + G* level of theory, the central angle (Si-N-Si) is calculated to be nearly linear (179.8°), in agreement with results of Bartmess and co-workers [72], who found a bond angle of 178.9° at the MP2/6-31 + G* level of theory. Interestingly, in contrast to previ-

ously reported results [72], our calculations at the MP2/6-31 + G* level of theory gave a geometry with a bond angle of 145.3° that is found to have all real force constants and therefore is calculated to be a true minimum on the potential energy surface. However, the MP2/6-31 + G*//B3LYP/6-31 + G* energy is only 0.4 kcal/mol higher than that of the calculated MP2 minimum, consistent with the assessment that the potential energy surface is very flat. The B3LYP/6-31 + G* frequencies for the very nearly linear structure were used for the data modeling, whereas the energy minima were used for energetics calculations.

The calculated values of the FSi(CH₃)₃ affinities examined in this work are included in Table 1. In general, slightly better agreement is found for the B3LYP/6-31 + G* results over the MP2/6-31 + G* results, although for *i*-propoxide, the measured value is essentially between the calculated values.

The fluorotrimethylsilane affinity has also been calculated for the silazide anion, (CH₃)₃SiNH⁻. Loss of FSi(CH₃)₃ from the fluoride adduct is calculated at the B3LYP/6-31 + G* level of theory to require 26.1 kcal/mol, as compared to a value of 35.7 kcal/mol at the MP2/6-31 + G* level of theory. The B3LYP value is in good agreement with the experimental value of 27.9 ± 1.8 kcal/mol obtained when using structure (**2d**) as the reactant ion (Table 2). Formation of hexamethyldisilazide by loss of HF from (**2d**) is calculated to require 31.2 kcal/mol at the B3LYP/6-31 + G* level of theory, 5 kcal/mol larger than the energy required for FSi(CH₃)₃ loss, whereas the MP2/6-31 + G* value for HF loss is 36.2 kcal/mol, only 0.5 kcal/mol higher than the barrier for silane loss. Therefore, whereas the B3LYP energy for loss of FSi(CH₃)₃ is in closer agreement with the experimental value, the MP2 prediction that the energies required for the two competing channels are similar is
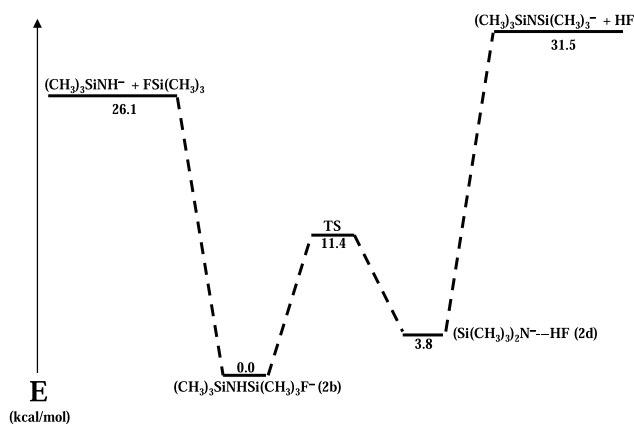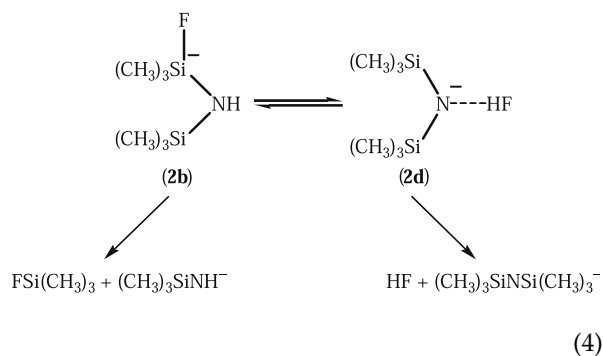
Figure 3. Potential energy diagram (in kcal/mol) for the decomposition of (CH$_3$)$_3$SiNHSi(CH$_3$)$_3$F$^-$. B3LYP/6-31 + G* relative enthalpies are indicated.

in better agreement with the experimental finding that the energy difference between the two points is small (Table 2).

From the calculated results, a potential energy surface for the dissociation of the HMDS/fluoride adduct is shown in Figure 3. As expected, the system consists of a double-well potential. The most important point on the surface is the transition state for the interconversion of (**2b**) and (**2d**), which is 11 kcal/mol higher than structure (**2b**). Therefore, structures (**2b**) and (**2d**) can interconvert rapidly at energies well below the required dissociation (eq 4) such that the initial composition of the ion mixture is not maintained. Because the reactant structures interconvert rapidly, FSi(CH$_3$)$_3$ can be lost by direct dissociation of (**2b**), whereas HF is formed by dissociation of (**2d**). This is in agreement with the experimental conclusion that both products are formed via loose transition states. This kinetic model for decomposition of (**2**) is analogous to the Curtin-Hammett principle [73, 74] familiar in physical-organic chemistry.

$$(4)$$

Discussion

In this section, we compare the measured silane affinities and consider additional derived thermochemical properties. In general, the silane affinities of the anions

reflect the gas-phase acidities of their conjugate acids. A plot of silane affinity vs. anion proton affinity is shown in Figure 4. In addition to the values measured in this work, we have included a CH$_3$$^-$ affinity to FSi(CH$_3$)$_3$, which can be derived from the fluoride affinity of tetramethylsilane [43]. A reasonable correlation is observed suggesting that the proton and FSi(CH$_3$)$_3$ share similar reactivity in terms of fundamental acid-base behavior. From the plot, we obtained an empirical linear relationship (eq 5) between the fluorotrimethylsilane affinity [SA(R$^-$)] and acidity of the conjugate acid of nucleophile R$^-$. This relationship can be used to predict other silane affinity values.

$$SA(R^-) = 0.36(\Delta H_{acid,298}(RH)) - 105.6 \quad (\text{in kcal/mol})$$

$$(5)$$

For example, given the acidity of water (390.3 kcal/mol) [77], the silane affinity of OH$^-$ is predicted to be ~35 kcal/mol, which agrees with the lower limit of 27 kcal/mol established from the reactivity of solvated OH$^-$ with FSi(CH$_3$)$_3$ [28]. On the other hand, using this relationship, the acidity of HF (371.3 kcal/mol) [77] suggests a fluoride affinity of 28 kcal/mol for FSi(CH$_3$)$_3$, well below the experimental value of 38 kcal/mol (or higher) [43]. Therefore, the relationship in eq 5 apparently does not apply to all substituents.

In some cases, the measured silane binding energies can also be used to determine fluoride affinities of the substituted silanes. The relationship between fluoride affinity (FA) and fluorotrimethylsilane affinity (eq 6, values at 298 K), shows that fluoride affinities can be derived for silanes with known enthalpies of formation.
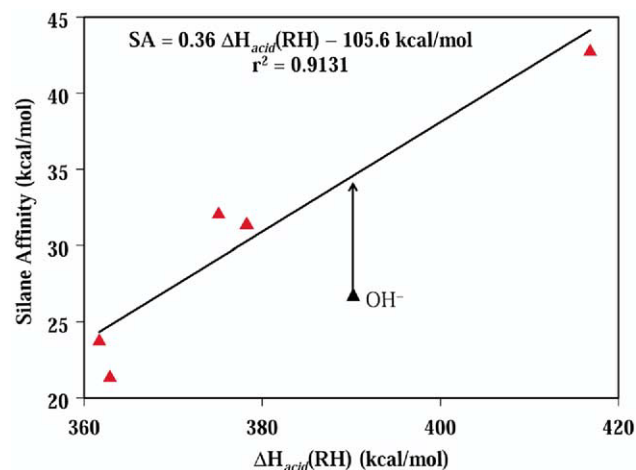
Figure 4. Plot of ΔH_{acid} values for RH versus experimentally determined nucleophilic affinities of R$^-$ to FSi(CH$_3$)$_3$ affinities. Six points are included, but only five are apparent because the data points for R = CH$_3$CH$_2$O- and (CH$_3$)$_3$SiNH- (modeled assuming structure **2b**) overlap. The start of the arrow is the lower limit for the hydroxide affinity of FSi(CH$_3$)$_3$ [28], and the arrowhead indicates an predicted value of ~35 kcal/mol.

Table 4. Experimental[a] and calculated[b] fluoride affinities (FA) for $RSi(CH_3)_3$ and the differences between $FA(RSi(CH_3)_3)$ and $DH_{298}(R^- - Si(CH_3)_3F)$

| R	Experimental FA	Calculated FA[b]	$FA(RSi(CH_3)_3)$ $-DH_{298}$ $(R^- -Si(CH_3)_3F)$
CH_3	29.9 ± 2.0[c]	N/A	-12.9
CH_3CH_2O	31.6 ± 2.0	33.4 (36.1)	$+0.2$
$(CH_3)_2CHO$	38.8 ± 2.4	33.3 (36.0)	$+7.4$
$(CH_3)_3SiO$	34.0 ± 4.9	34.4 (38.0)	$+12.6$
$(CH_3)_3SiNH$[d]			
(**2b**)	36 ± 7	34.5 (37.0)	$+5$
(**2d**)	33 ± 7	30.7 (30.7)	$+5$
CF_3CH_2O	N/A[e]	44.5 (47.3)	$+22.9$ $(+16.6)$[f]

[a]Values in kcal/mol, derived from eq 6.
[b]B3LYP/6-31 + G* and (MP2/6-31 + G*) values as discussed in the text.
[c]Reference [43].
[d]The results depend on the structure assumed for the reactant ion, (**2b**) or (**2d**). Both results are reported (see Table 2 and text).
[e]This value could not be derived (no ΔH_f value available).
[f]Computed value at B3LYP/6-31+G* and (MP2/6-31 + G*).

$$DH_{298}(RSi(CH_3)_3) - F^-) = \Delta H_{acid}(HF)$$
$$- \Delta H_{acid}(RH) + DH_{298}(R^- - Si(CH_3)_3F)$$
$$+ \Delta H_f(RSi(CH_3)_3)$$
$$+ \Delta H_f(HF) - \Delta H_f(RH) - \Delta H_f(FSi(CH_3)_3)$$
$$= DH_{298}(R^- - Si(CH_3)_3F)$$
$$+ \Delta H_f(RSi(CH_3)_3) - \Delta H_{acid}(RH) - \Delta H_f(RH)$$
$$+ 441.8 \pm 0.2 \text{ kcal/mol} \qquad (6)$$

Derived fluoride affinities are listed in Table 4. In general, the measured fluoride affinities are in good agreement with calculated values. In the case of HMDS, thermochemical values had to be examined closely. Initially, incorporation of the literature values of $\Delta H_{acid}[(CH_3)_3SiNH_2]$, $\Delta H_f[(CH_3)_3SiNH_2]$, or $\Delta H_f[(CH_3)_3SiNHSi(CH_3)_3]$ resulted in large deviation from the calculated value of the fluoride affinity. Of these three values, $\Delta H_{acid}[(CH_3)_3SiNH_2]$ and $\Delta H_f[(CH_3)_3SiNHSi(CH_3)_3]$ were determined experimentally, whereas $\Delta H_f[(CH_3)_3SiNH_2]$ has only been indirectly estimated (-69.6 kcal/mol) [50]. In light of this, we have re-evaluated this value with existing thermochemistry. Using an isodesmic approach (eq 7), the calculated enthalpy of the reaction is $+2.1$ kcal/mol (B3LYP/6-31 + G* level of theory).

$$(CH_3)_3SiNH_2 + (CH_3)_3SiN(CH_3)_2 \rightarrow$$
$$2(CH_3)_3SiNH(CH_3) \qquad (7)$$
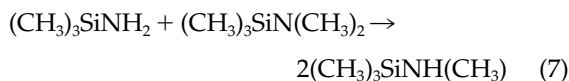
The small value for the calculated enthalpy of this reaction suggests that the enthalpy of formation of $(CH_3)_3SiNH_2$ can be reliably estimated by using a bond additivity approach. Using the measured enthalpies of formation of $(CH_3)_3SiN(CH_3)_2$ and $(CH_3)_3SiNH(CH_3)$ [78], shown in Table 5, an estimated value of -49 ± 3 kcal/mol is obtained for $\Delta H_f[(CH_3)_3SiNH_2]$. The uncertainty is assigned to account for a potential 2 kcal/mol deviation from bond additivity suggested by the elec-

tronic structure calculations. The derived value is significantly lower than previous estimates by Becerra and Walsh (-69.6 kcal/mol) [50], Luo and Benson (-69.1 kcal/mol) [79], and Leroy et al. (-62.7 kcal/mol) [80]. However, if we include the additivity value with the experimental data, then the fluoride affinity of $(CH_3)_3SiNHSi(CH_3)_3$ is 36 ± 7 kcal/mol [assuming structure (**2b**)], or 33 ± 7 kcal/mol [assuming structure (**2d**)]. These values are in closer agreement with computational predictions of the fluoride affinity (31–37

Table 5. Supplemental thermochemical parameters used in this study[a]

Species	$\Delta H_f(kcal/mol)$[b]	$\Delta H_{acid}(kcal/mol)$[b]
$FSi(CH_3)_3$	-135.8[c]	—
$CH_3CH_2OSi(CH_3)_3$	-119.3 ± 1.2[d]	—
$CF_3CH_2OSi(CH_3)_3$	Not available	—
$(CH_3)_2CHOSi(CH_3)_3$	-125.2 ± 1.2[d]	—
$(CH_3)_3SiOSi(CH_3)_3$	-185.8 ± 1.4[e]	—
$(CH_3)_3SiNHSi(CH_3)_3$	-107.7 ± 2.4[e]	356.0 ± 2.3[f]
$(CH_3)_3SiNH(CH_3)$	-54.3 ± 1.0[c]	—
$(CH_3)_3SiN(CH_3)_2$	-59.3 ± 1.0[c]	—
$Si(CH_3)_4$	-55.7 ± 0.9[g]	—
HF	-65.3 ± 0.2	371.3
CH_3CH_2OH	-56.2 ± 0.1	378.3 ± 1.0
CF_3CH_2OH	-212.4 ± 0.2[h]	361.7 ± 2.5
$(CH_3)_2CHOH$	-65.2	375.1 ± 1.0
$(CH_3)_3SiOH$	-119.5 ± 0.7[c]	362.9 ± 4.6
$(CH_3)_3SiNH_2$	-51.4 ± 3.0[i]	378.2 ± 5.1
H_2O	—	390.3
H_2	—	400.4
CH_4	-17.9	416.8 ± 0.7

[a]Additional required thermochemical parameters were $DH_{298}(H-H) = 104.2$ kcal/mol [81] and IP(H) = 313.6 kcal/mol.
[b]Gas phase enthalpies at 298 K; values from NIST Web Book [77] unless otherwise marked. Significant uncertainties are stated where indicated.
[c]Reference [50].
[d]Reference [82].
[e]Reference [83].
[f]Reference [49].
[g]Reference [84].
[h]Derived from NIST Web Book [77] data where $\Delta H_f(CF_3H_2OH(g)) = \Delta H_f(CF_3H_2OH(l)) + \Delta H_{vap}(CF_3H_2OH(l))$.
[i]Derived value as described in text.

kcal/mol, Table 4) than would be obtained when using the previously reported values. For example, using the value of −69.6 kcal/mol reported by Becerra and Walsh leads to a fluoride affinity of ca. 57 kcal/mol, significantly higher than the calculated value, and is, moreover, significantly higher than any previously reported value for a trimethylsilane [77]. The fluoride affinity derived from the revised enthalpy of formation is in the range of those reported previously for these types of systems [77]. It should also be added that all of these experimental fluoride affinities depend upon a recommended value for the enthalpy of formation of fluorotrimethylsilane [50].

Combination of the fluorotrimethylsilane affinity of the anion and the fluoride affinity of the silane provides insight into the desilylation reaction. For fluoride-induced desilylation to occur in the gas phase, the fluoride affinity of the silane must be larger than the silane affinity of R⁻. The differences between fluoride and silane affinities are shown in Table 4. Fluoride-induced desilylation is found to be thermochemically allowed with all of the silanes examined in this work, albeit marginally for ethoxytrimethylsilane. Therefore, alkoxide ion formation by fluoride-induced desilylation is shown to be thermochemically viable, consistent with the observed reactivity [7]. Similarly, the difference between the FA of tetramethylsilane and the FSi(CH₃)₃ affinity of methide is ~13 kcal/mol, consistent with the observation that the only observed reactions between fluoride and TMS are adduct formation (94%) and proton transfer (6%) [7]. Damrauer and co-workers have previously addressed the general importance of the balance between the affinity of the silane to the incoming anion and the leaving group [29].

Conclusions

Collision-induced dissociation studies of pentavalent siliconates have been used to assess thermochemistry of fluoride-induced desilylation reactions. Although the thermochemistry can usually be calculated for enthalpies of formation and gas-phase acidities, the combination of fluoride and silane affinities can be used to assess cases where gas-phase acidities are not known. Our results indicate that fluorotrimethylsilane affinities of ions generally track the ion proton affinities, accounting for the observations that more basic ions are more difficult to generate by fluoride-induced desilylation.

Acknowledgments

References

1. Larson, G. L. Recent Synthetic Applications of Organosilanes. In *The Chemistry of Organic Silicon Compounds*; Rappoport, Z.; Patai, S., Eds.; John Wiley and Sons: Chichester, UK, 1989; pp 763–808.
2. Jung, M. E.; Lyster, M. A. Quantitative Dealkylation of Alkyl Ethers via Treatment with Trimethylsilyl Iodide. A New Method for Ether Hydrolysis. *J. Org. Chem.* **1977,** *42,* 3761–3764.
3. Olah, G. A.; Narang, S. C.; Gupta, B. G. B.; Malhotra, R. Synthetic Methods and Reactions. 62. Transformation with Chlorotrimethylsilane/Sodium Iodide, a Convenient in Situ Iodotrimethylsilane Reagent. *J. Org. Chem.* **1979,** *44,* 1247–1251.
4. Danishefsky, S.; Hungate, R. J. The Total Synthesis of Octosyl Acid A: A New Departure in Organostannylene Chemistry. *J. Am. Chem. Soc.* **1986,** *108,* 2486–2487.
5. Harpp, D. N.; Gingras, M. Fluorodestannylation. A Powerful Technique to Liberate Anions of Oxygen, Sulfur, Selenium, and Carbon. *J. Am. Chem. Soc.* **1988,** *110,* 7737–7745.
6. DePuy, C. H.; Bierbaum, V. M.; Flippin, L. A.; Grabowski, J. J.; King, G. K.; Schmitt, R. J. Generation of Specific Isomeric Carbanions in the Gas Phase. *J. Am. Chem. Soc.* **1979,** *101,* 6443.
7. DePuy, C. H.; Bierbaum, V. M.; Flippin, L. A.; Grabowski, J. J.; King, G. K.; Schmitt, R. J.; Sullivan, S. A. Gas-Phase Reactions of Anions with Substituted Silanes. *J. Am. Chem. Soc.* **1980,** *102,* 5012–5015.
8. Broadus, K. M.; Han, S.; Kass, S. R. Rearrangements of 3-Aryl-Substituted Cyclopropenyl Anions and the Gas-Phase Acidity of 3-(4-Methylphenyl)Cyclopropene. *J. Org. Chem.* **2001,** *66,* 99–106.
9. Hammad, L. A.; Wenthold, P. G. Triradical Thermochemistry from Collision-Induced Dissociation Threshold Energy Measurements. The Heat of Formation of 1,3,5-Trimethylenebenzene. *J. Am. Chem. Soc.* **2001,** *123,* 12311–12317.
10. Reed, D. R.; Kass, S. R.; Mondanaro, K. R.; Dailey, W. P. Formation of a 1-Bicyclo[1.1.1]Pentyl Anion and an Experimental Determination of the Acidity and C—H Bond Dissociation Energy of 3-*tert*-Butylbicyclo[1.1.1]Pentane. *J. Am. Chem. Soc.* **2002,** *124,* 2790–2795.
11. Schwarz, H. Positive and Negative Ion Chemistry of Silicon-Containing Molecules in the Gas Phase. In *The Chemistry of Organic Silicon Compounds*; Rappoport, Z.; Patai, S., Eds.; John Wiley and Sons: Chichester, UK, 1989; pp 445–510.
12. Hare, M. C.; Marimanikkuppam, S. S.; Kass, S. R. Acetamide Enolate: Formation, Reactivity, and Proton Affinity. *Int. J. Mass Spectrom.* **2001,** *210/211,* 153–163.
13. Sachs, R. K.; Kass, S. R. 3-Carbomethoxycyclopropen-3-yl Anion. Formation and Characterization of an Antiaromatic Ion. *J. Am. Chem. Soc.* **1994,** *116,* 783–784.
14. Hare, M.; Emrick, T.; Eaton, P. E.; Kass, S. R. Cubyl Anion Formation and an Experimental Determination of the Acidity and C—H Bond Dissociation Energy of Cubane. *J. Am. Chem. Soc.* **1997,** *119,* 237–238.
15. DePuy, C. H.; Damrauer, R. Reactions of Organosilicon Anionic Species with Nitrous Oxide. *Organometallics* **1984,** *3,* 362–365.
16. Brinkman, E. A.; Berger, S.; Brauman, J. I. α-Silyl-Substituent Stabilization of Carbanions and Silyl Anions. *J. Am. Chem. Soc.* **1994,** *116,* 8304–8310.
17. Wenthold, P. G.; Hu, J.; Squires, R. R. Regioselective Synthesis of Biradical Negative Ions in the Gas Phase. Generation of Trimethylenemethane, *m*-Benzyne, and *p*-Benzyne Anions. *J. Am. Chem. Soc.* **1994,** *116,* 6961–6962.
18. Wenthold, P. G.; Hu, J.; Squires, R. R. *o*-, *m*-, and *p*-Benzyne Negative Ions in the Gas Phase: Synthesis, Authentication, and Thermochemistry. *J. Am. Chem. Soc.* **1996,** *118,* 11865–11871.

19. Wenthold, P. G.; Hu, J.; Hill, B. T.; Squires, R. R. Gas-Phase Negative Ion Chemistry of Molecular Fluorine. Synthesis of Distonic Radical Anions and Related Species. *Int. J. Mass Spectrom.* **1998,** *179/180,* 173–183.

20. Lardin, H. A.; Nash, J. J.; Wenthold, P. G. Is the 1,3,5-Tridehydrobenzene Triradical a Cyclopropenyl Radical Analog? *J. Am. Chem. Soc.* **2002,** *124,* 12612–12618.

21. Munsch, T. E.; Slipchenko, L. V.; Krylov, A. I.; Wenthold, P. G. Reactivity and Structure of the 5-Dehydro-*m*-Xylylene Anion. *J. Org. Chem.* **2004,** *69,* 5735–5741.

22. Slipchenko, L. V.; Munsch, T. E.; Wenthold, P. G.; Krylov, A. I. 5-Dehydro-1,3-Quinodimethane: A Hydrocarbon with an Open-Shell Doublet Ground State. *Angew. Chem. Int. Ed.* **2004,** *43,* 742–745.

23. Bassindale, A. R.; Glynn, S. J.; Taylor, P. G. Reaction Mechanisms of Nucleophilic Attack at Silicon. In *The Chemistry of Organic Silicon Compounds*; Rappoport, Z.; Apeloig, Y., Eds.; Wiley: Chichester, 1998; pp 495–512.

24. Musher, J. I. Chemistry of Hypervalent Molecules. *Angew. Chem. Int. Ed. Engl.* **1969,** *8,* 54–68.

25. Hajdasz, D. J.; Ho, Y.; Squires, R. R. Gas-Phase Chemistry of Pentacoordinate Silicon Hydride Ions. *J. Am. Chem. Soc.* **1994,** *116,* 10751–10760.

26. Hajdasz, D. J.; Squires, R. R. Hypervalent Silicon Hydrides: SiH$_5^-$. *J. Am. Chem. Soc.* **1986,** *108,* 3139–3140.

27. Krouse, I. H.; Lardin, H. A.; Wenthold, P. G. Gas-Phase Ion Chemistry and Ion Thermochemistry of Phenyltrifluorosilane. *Int. J. Mass Spectrom.* **2003,** *227,* 303–314.

28. Krouse, I. H.; Wenthold, P. G. Formation and Decomposition of Hydroxysiliconates in the Gas Phase. *Organometallics* **2004,** *23,* 2573–2582.

29. Damrauer, R.; Burggraf, L. W.; Davis, L. P.; Gordon, M. S. Gas-Phase and Computational Studies of Pentacoordinate Silicon. *J. Am. Chem. Soc.* **1988,** *110,* 6601–6606.

30. Kira, M.; Sato, K.; Sakurai, H. Pentacoordinate Allylsilicates: Characterization and Highly Stereoselective Reaction with Aldehydes. *J. Am. Chem. Soc.* **1988,** *110,* 4599–4602.

31. Becker, B.; Corriu, R. J. P.; Guérin, C.; Henner, B. J. L. Hypervalent Silicon Hydrides: Evidence for Their Intermediacy in the Exchange Reactions of Di- and Tri-Hydrogenosilanes Catalyzed by Hydrides (NaH, KH, and LiAlH$_4$). *J. Organomet. Chem.* **1989,** *369,* 147–154.

32. Holmes, R. R. The Stereochemistry of Nucleophilic Substitution at Tetracoordinated Silicon. *Chem. Rev.* **1990,** *90,* 17–31.

33. Gordon, M. S.; Davis, L. P.; Burggraf, L. W.; Damrauer, R. Theoretical Studies of the Reactions XH$_n$ → XH$_{n-1}^-$ + H$^+$ and XH$_{n-1}^-$ + SiH$_4$ → [SiH$_4$XH$_{n-1}$]$^-$. *J. Am. Chem. Soc.* **1986,** *108,* 7889–7893.

34. Deiters, J. A.; Holmes, R. R. Pathways for Nucleophilic Substitution at Silicon. A Molecular Orbital Approach. *J. Am. Chem. Soc.* **1987,** *109,* 1686–1692.

35. DePuy, C. H.; Damrauer, R.; Bowie, J. H.; Sheldon, J. C. Gas-Phase Negative Ion Chemistry of Organosilanes. *Acc. Chem. Res.* **1987,** *20,* 127–133.

36. Damrauer, R.; Kass, S. R.; DePuy, C. H. Gas-Phase Acidities of Methylsilanes: C-H versus Si-H. *Organometallics* **1988,** *7,* 637–640.

37. da Silva, M. L. P.; Riveros, J. M. Gas-Phase Nucleophilic Reactions in Tetraalkoxysilanes. *J. Mass Spectrom.* **1995,** *30,* 733–740.

38. Sheldon, J. C.; Hayes, R. N.; Bowie, J. H. Do Barriers Exist for Nucleophilic Substitution at Tetravalent Silicon in the Gas Phase? An ab Initio and Ion Cyclotron Resonance Study. *J. Am. Chem. Soc.* **1984,** *106,* 7711–7715.

39. Sheldon, J. C.; Hayes, R. N.; Bowie, J. H.; DePuy, C. H. The Mechanisms of Alkane Eliminations from the Intermediates Produced by Reactions of the Hydroxide and Methoxide Negative Ions with Tetramethylsilane in the Gas Phase. *J. Chem. Soc. Perkin Trans. II* **1987,** 275–280.

40. Wong, J.; Sannes, K. A.; Johnson, C. E.; Brauman, J. I. Energetics and Mechanism of Alkyl Cleavage Transition States: Relative Gas-Phase Acidities of Alkanes. *J. Am. Chem. Soc.* **2000,** *122,* 10878–10885.

41. Veszpremi, T.; Harada, Y.; Ohno, K.; Mutoh, H. J. Photoelectron and Penning Electron Spectroscopic Investigation of Phenylhalosilanes. *J. Organomet. Chem.* **1984,** *266,* 9–16.

42. Afeefy, H. Y.; Liebman, J. F.; Stein, S. E. Neutral Thermochemical Data. In *NIST Chemistry WebBook, NIST Standard Reference Database Number 69*; Mallard, W. G.; Linstrom, P. J., Eds.; National Institute of Standards and Technology: Gaithersburg, MD, March 2003.

43. Larson, J. W.; McMahon, T. B. Fluoride and Chloride Affinities of Main Group Oxides, Fluorides, Oxofluorides, and Alkyls. Quantitative Scales of Lewis Acidities from Ion Cyclotron Resonance Halide-Exchange Equilibria. *J. Am. Chem. Soc.* **1985,** *107,* 766–773.

44. Murphy, M. K.; Beauchamp, J. L. Methyl and Fluorine Substituent Effects on the Gas Phase Lewis Acidities of Silanes by ICR Spectroscopy. *J. Am. Chem. Soc.* **1977,** *99,* 4992–4999.

45. van der Wel, H.; Nibbering, N. M. M.; Sheldon, J. C.; Hayes, R. N.; Bowie, J. H. Nucleophilic Substitution in the Gas Phase. The Reactions of Alkoxide-Alkanol Negative Ions with Boron, Carbon, Silicon, and Titanium Alkoxides. An Ion Cyclotron Resonance and ab Initio Study. *J. Am. Chem. Soc.* **1987,** *109,* 5823–5828.

46. DePuy, C. H.; Gronert, S.; Mullin, A.; Bierbaum, V. M. Gas-Phase S$_N$2 and E2 Reactions of Alkyl Halides. *J. Am. Chem. Soc.* **1990,** *112,* 8650–8655.

47. Damrauer, R.; Simon, R.; Krempp, M. Effect of Substituents on the Gas-Phase Acidity of Silanols. *J. Am. Chem. Soc.* **1991,** *113,* 4431–4435.

48. O'Hair, R. A. J.; Krempp, M.; Damrauer, R.; DePuy, C. H. Gas-Phase Ion Chemistry of HP$_2^-$, FP$_2^-$, and HP$_2^+$. *Inorg. Chem.* **1992,** *31,* 2092–2096.

49. Grimm, D. T.; Bartmess, J. E. Intrinsic (Gas-Phase) Basicity of Some Anionic Bases Commonly Used in Condensed-Phase Synthesis. *J. Am. Chem. Soc.* **1992,** *114,* 1227–1231.

50. Becerra, R.; Walsh, R. Thermochemistry. In *The Chemistry of Organic Silicon Compounds*; Rappoport, Z.; Apeloig, Y., Eds. John Wiley and Sons: Chichester, UK, 1998; pp 153–180.

51. Buckingham, J. Dictionary of Organic Compounds; Chapman and Hall: New York, 1982.

52. Sauer, R. O. Derivatives of the Methylchlorosilanes. I. Trimethylsilanol and Its Simple Ethers. *J. Am. Chem. Soc.* **1944,** *66,* 1707–1710.

53. Pinnick, H. W.; Bal, B. S.; Lajis, N. H. A New Preparation of Trimethylsilyl Ethers. *Tetrahedron Lett.* **1978,** *19,* 4261–4262.

54. Nakano, T.; Ohkawa, K.; Matsumoto, H.; Nagai, Y. Convenient Synthesis of Aromatic Acid Chlorides. The Reaction of Benzylidyne Chlorides with Hexamethyldisiloxane. *J. Chem. Soc. Chem. Commun.* **1977,** 808–809.

55. Welsch, T.; Müller, R.; Engewald, W.; Werner, G. Surface Modification of Glass Capillaries by High-Temperature Silylation. *J. Chromatogr. A* **1982,** *241,* 41–48.

56. Graul, S. T.; Squires, R. R. Advances in Flow Reactor Techniques for the Study of Gas-Phase Ion Chemistry. *Mass Spectrom. Rev.* **1988,** *7,* 263–358.

57. Marinelli, P. J.; Paulino, J. A.; Sunderlin, L. S.; Wenthold, P. G.; Poutsma, J. C.; Squires, R. R. A Tandem Selected Ion Flow Tube-Triple Quadrupole Instrument. *Int. J. Mass Spectrom. Ion Processes* **1994,** *130,* 89–105.

58. Bickelhaupt, F. M.; de Koning, L. J.; Nibbering, N. M. M. Anionic Ether Cleavage of Tetrahydrofuran in the Gas Phase. *Tetrahedron* **1993,** *49,* 2077–2092.

59. Ervin, K. M.; Armentrout, P. B. Translational Energy Dependence of Ar$^+$ + XY → ArX$^+$ + Y (XY = H$_2$, D$_2$, HD) from Thermal to 30 eV c.m. *J. Chem. Phys.* **1985,** *83,* 166–189.

60. Schultz, R. H.; Crellin, K. C.; Armentrout, P. B. Sequential Bond Energies of Iron Carbonyl Fe(CO)$_x$$^+$ (x = 1–5): Systematic Effects on Collision-Induced Dissociation Measurements. *J. Am. Chem. Soc.* **1991,** *113,* 8590–8601.

61. Sunderlin, L. S.; Armentrout, P. B. Thermochemistry of Titanium(1+)-Hydrocarbon Bonds: Translational Energy Dependence of the Reactions of Ti$^+$ with Ethane, Propane, and trans-2-Butene. *Int. J. Mass Spectrom. Ion Processes* **1989,** *94,* 149–177.

62. Chesnavich, W. J.; Bowers, M. T. Theory of Translationally Driven Reactions. *J. Phys. Chem.* **1979,** *83,* 900–905.

63. Ervin, K. M. Experimental Techniques in Gas-Phase Ion Thermochemistry. *Chem. Rev.* **2001,** *101,* 391–444.

64. Muntean, F.; Armentrout, P. B. Guided Ion Beam Study of Collision-Induced Dissociation Dynamics: Integral and Differential Cross Sections. *J. Chem. Phys.* **2001,** *115,* 1213–1228.

65. Rodgers, M. T.; Ervin, K. M.; Armentrout, P. B. Statistical Modeling of Collision-Induced Dissociation Thresholds. *J. Chem. Phys.* **1997,** *106,* 4499–4508.

66. Rodgers, M. T.; Armentrout, P. B. Statistical Modeling of Competitive Threshold Collision-Induced Dissociation. *J. Chem. Phys.* **1998,** *109,* 1787–1800.

67. Dalleska, N. F.; Honma, K.; Sunderlin, L. S.; Armentrout, P. B. Solvation of Transition Metal Ions by Water. Sequential Binding Energies of M$^+$(H$_2$O)$_x$ (x = 1–4) for M = Ti to Cu Determined by Collision-Induced Dissociation. *J. Am. Chem. Soc.* **1994,** *116,* 3519–3528.

68. Holfter, H.; Kirchmeier, R. L.; Shreeve, J. M. Insertion of γ-SO$_3$ into Perfluoroalkyl- and Polyfluoroalkoxysilanes. *Inorg. Chem.* **1994,** *33,* 6369–6372.

69. Frisch, M. J.; Trucks, G. W.; Schlegel, H. B.; Scuseria, G. E.; Robb, M. A.; Cheeseman, J. R.; Montgomery, J. A., Jr.; Vreven, T.; Kudin, K. N.; Burant, J. C.; Millam, J. M.; Iyengar, S. S.; Tomasi, J.; Barone, V.; Mennucci, B.; Cossi, M.; Scalmani, G.; Rega, N.; Petersson, G. A.; Nakatsuji, H.; Hada, M.; Ehara, M.; Toyota, K.; Fukuda, R.; Hasegawa, J.; Ishida, M.; Nakajima, T.; Honda, Y.; Kitao, O.; Nakai, H.; Klene, M.; Li, X.; Knox, J. E.; Hratchian, H. P.; Cross, J. B.; Adamo, C.; Jaramillo, J.; Gomperts, R.; Stratmann, R. E.; Yazyev, O.; Austin, A. J.; Cammi, R.; Pomelli, C.; Ochterski, J. W.; Ayala, P. Y.; Morokuma, K.; Voth, G. A.; Salvador, P.; Dannenberg, J. J.; Zakrzewski, V. G.; Dapprich, S.; Daniels, A. D.; Strain, M. C.; Farkas, O.; Malick, D. K.; Rabuck, A. D.; Raghavachari, K.; Foresman, J. B.; Ortiz, J. V.; Cui, Q.; Baboul, A. G.; Clifford, S.; Cioslowski, J.; Stefanov, B. B.; Liu, G.; Liashenko, A.; Piskorz, P.; Komaromi, I.; Martin, R. L.; Fox, D. J.; Keith, T.; Al-Laham, M. A.; Peng, C. Y.; Nanayakkara, A.; Challacombe, M.; Gill, P. M. W.; Johnson, B.; Chen, W.; Wong, M. W.; Gonzalez, C.; Pople, J. A. *Gaussian 03, Revision B.05*; Gaussian, Inc., Pittsburgh, PA, 2003.

70. Damrauer, R.; Hankin, J. A. Chemistry and Thermochemistry of Silicon-Containing Anions in the Gas Phase. *Chem. Rev.* **1995,** *95,* 1137–1160.

71. Tumas, W.; Salomon, K. E.; Brauman, J. I. Dimethylsilanone Enolate Anion: Competitive Fragmentation and Electron Autodetachment of Vibrationally Excited Siloxide Anions in the Gas Phase. *J. Am. Chem. Soc.* **1986,** *108,* 2541–2546.

72. Higgins, P. R.; Hinde, R. J.; Grimm, D. T.; Bloor, J. E.; Bartmess, J. E. The Geometric Dependence of Acidity: Hexamethyldisilazide Anion. *Int. J. Mass Spectrom.* **2001,** *210/211,* 231–240.

73. Curtin, D. Y. Stereochemical Control of Organic Reaction. Differences in Behavior of Diastereoisomers. I. Ethane Derivative. The cis Effect. *Rec. Chem. Prog.* **1954,** *15,* 111–128.

74. Seeman, J. I. Effect of Conformational Change on Reactivity in Organic Chemistry. Evaluations, Application, and Extensions of Curtin-Hammett/Winstein-Holness Kinetics. *Chem. Rev.* **1983,** *83,* 83–134.

75. Broadus, K. M.; Kass, S. R.; Osswald, T.; Prinzbach, H. Dodecahedryl Anion Formation and an Experimental Determination of the Acidity and C—H Bond Dissociation Energy of Dodecahedrane. *J. Am. Chem. Soc.* **2000,** *122,* 10964–10968.

76. Damrauer, R.; Crowell, A. J.; Craig, C. F. Electron, Hydride, and Fluoride Affinities of Silicon-Containing Species: Computational Studies. *J. Am. Chem. Soc.* **2003,** *125,* 10759–10766.

77. Linstrom, P. J.; Mallard, W. D., Eds., NIST Chemistry Web-Book, NIST Standard Reference Database Number 69. National Institute of Standards and Technology, Gaithersburg MD, March 2003.

78. Baldwin, J. C.; Lappert, M. F.; Pedley, J. B.; Treverton, J. A. Bonding Studies of Organometallic Compounds of Boron and the Group IV Elements. Part I. Heats of Hydrolysis and Bond Energies for Some Trimethylsilyl Derivatives. *J. Chem. Soc. A* **1967,** 1980–1984.

79. Luo, Y.; Benson, S. W. New Eletronegativity Scale for the Correlation of Heats of Formation and Bond Dissociation Energies. 6. Alkylsilane Derivatives. *J. Phys. Chem.* **1989,** *93,* 4643–4645.

80. Leroy, G.; Riffi Temsamani, D.; Wilante, C. Refinement and Extension of the Table of Standard Energies for Bonds Containing Atoms of the Fourth Group of the Periodic Table. *J. Mol. Struct. Theochem.* **1994,** *306,* 21–39.

81. Blanksby, S. J.; Ellison, G. B. Bond Dissociation Energies of Organic Molecules. *Acc. Chem. Res.* **2003,** *36,* 255–263.

82. Voronkov, M. G.; Baryshok, V. P.; Klyuchnikov, V. A.; Danilova, T. F.; Pepekin, V. I.; Korchagina, A. N.; Khudobin, Y. I. Thermochemistry of Organosilicon Compounds. I. Triorganyl-, Tetraorganyl-, Organylorganoxy-, and Tetraorganoxy-Silanes. *J. Organomet. Chem.* **1988,** *345,* 27–38.

83. Baldwin, J. C.; Lappert, M. F.; Pedley, J. B.; Poland, J. S. Bonding Studies of Compounds of Boron and the Group IV Elements. Part VIII. Heats of Hydrolysis and Bond Energies for Some Trimethylmetalyl Derivatives Me$_3$M-X (M = Si, Ge, and Sn). *J. Chem. Soc. Dalton Trans.* **1972,** 1943–1947.

84. Steele, V. W. The Standard Molar Enthalpies of Formation of Organo-Silicon Compounds and Related Bond-Dissociation Enthalpies. 2. Tetramethylsilane. *J. Thermodyn.* **1983,** 595–601.